JOURNAL OF AIRCRAFT
Vol. 41, No. 1, January–February 2004

Engineering Notes

ENGINEERING NOTES are short manuscripts describing new developments or important results of a preliminary nature. These Notes cannot exceed 6 manuscript pages and 3 figures; a page of text may be substituted for a figure and vice versa. After informal review by the editors, they may be published within a few months of the date of receipt. Style requirements are the same as for regular contributions (see inside back cover).

Unsteady Pressures Associated with Vortical Flows and Forced Oscillation

Robert C. Scott,* Walter A. Silva,† James R. Florance,‡ and Donald F. Keller§
NASA Langley Research Center, Hampton, Virginia 23681

Introduction

A goal of the Transonic Dynamics Tunnel (TDT)[1,2] at the NASA Langley Research Center is to acquire high-quality wind-tunnel data for the validation of aeroelastic analysis methods including the development and application of aeroelastic computational fluid dynamics (CFD) codes. The need for such data has been recognized for many years and has led to the development of various programs to generate a database of high-quality unsteady data. The RTO effort[3] is an example of an international cooperative effort to define, compile, and disseminate high-quality experimental data sets. A NASA Langley effort was the Benchmark Models Program (BMP). The BMP resulted in the testing of several configurations for which steady and unsteady pressures and flutter data were obtained.[4–8] Testing of the benchmark active controls technology model[9] comprises the most recent data set for this class of wind-tunnel models.

The rigid semispan model (RSM), the focus of this paper, and an identically shaped flexible version[10] of the RSM were defined near the end of NASA Langley's BMP. These wind-tunnel models, intended to be representative of a high-speed civil transport (HSCT), became part of the aeroelasticity element of the high-speed research (HSR) program.

Six separate wind-tunnel tests of the RSM were conducted using three different mount systems. Reference 11 provides a description of all of the RSM tests. The final three of these tests yielded the best quality data with each of these three tests using separate mounting systems: a 5-degree-of-freedom (DOF) balance, a 2-DOF pitch and plunge apparatus (PAPA), and an oscillating turntable (OTT). The primary purpose of this Note is to describe the OTT database and present samples of steady and unsteady pressure data. Where applicable, comparisons will be made between OTT data and data acquired on previous wind-tunnel tests. Additionally, CFD results will be compared with experimental data. Discussion of the data and results will demonstrate that the RSM database provides significant challenges for verification and validation of CFD codes.

Presented as Paper 2002-1648 at the AIAA/ASME/ASCE/AHS/ASC 43rd Structural Dynamics and Materials Conference, Denver, CO, 22 April 2002; received 31 July 2002; revision received 25 August 2003; accepted for publication 26 August 2003. This material is declared a work of the U.S. Government and is not subject to copyright protection in the United States. Copies of this paper may be made for personal or internal use, on condition that the copier pay the $10.00 per-copy fee to the Copyright Clearance Center, Inc., 222 Rosewood Drive, Danvers, MA 01923; include the code 0021-8669/04 $10.00 in correspondence with the CCC.

*Senior Aerospace Engineer, Aeroelasticity Branch. Associate Fellow AIAA.
†Senior Research Scientist, Aeroelasticity Branch. Associate Fellow AIAA.
‡Aerospace Engineer, Aeroelasticity Branch. Senior Member AIAA.
§Senior Aerospace Engineer, Aeroelasticity Branch.

Experimental Apparatus

RSM

The RSM planform is a $\frac{1}{12}$-scale configuration based on an early design known as the Reference H configuration. Model airfoil shapes were based on those of Reference H, with the model wing thickness being increased to a constant 4% thickness-to-chord ratio to accommodate pressure instrumentation at the wing tip. The model was designed to be very stiff to allow the measurement of aerodynamic properties without the effects of structural deformations.

Figure 1 shows the planform layout and main components of the RSM including the three primary mounts used during the various wind-tunnel tests. The leading and trailing edges were removable to access pressure instrumentation in those regions. A removable tip cap allowed access to pressure instrumentation at the wing tip. The RSM could be tested with and without a pair of flow-through nacelles. The nacelles were rigidly attached to pylons on the lower, inboard surface of the wing. The RSM wing had a graphite epoxy composite structure with an open-cell foam core.

The RSM was tested with a rigid fuselage fairing, which displaced the model away from the wind-tunnel wall boundary layer while serving as an aerodynamic boundary condition at the wing root. Additionally, the rigid fuselage fairing provided an aerodynamic shield for the hardware, instrumentation, and wire bundles located at the wing root. Three different fuselage fairings were used with the RSM. The lengths of these fuselage fairings were approximately 18, 14, and 11 ft. The 14-ft fuselage was used on both the PAPA and OTT tests.

The instrumentation layout for the RSM (visible in Fig. 1) consisted of 131 in situ unsteady pressure transducers located at the 10, 30, 60, and 95% span stations. Six additional unsteady pressure transducers were installed at the 20% chord station for the 20, 45, and 75% span stations for both upper and lower surfaces. Channels were carved into the foam core to accommodate the wiring for the instrumentation. Instrumentation also included accelerometers installed throughout the wing. The

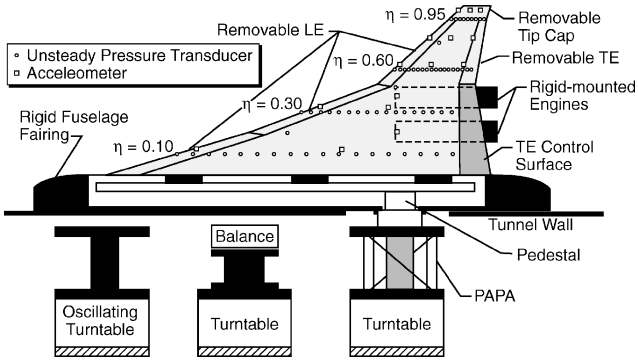

Fig. 1 Planform, model details, and instrumentation layout for the RSM wind-tunnel model.

14-ft-long fuselage fairing was instrumented with unsteady pressure transducers.

A remotely commanded, hydraulically actuated control surface was available on the RSM. This flap was capable of rotating ±15 deg without the engine nacelles installed. When installed, the inboard engine nacelle inhibited downward motion of the trailing-edge flap. The flap was used to obtain unsteady aerodynamic data on the balance and PAPA mount systems.

Oscillating Turntable

The RSM was the first model to be tested using the TDT's new OTT. The OTT is essentially a very large hydraulic actuator that can be used to oscillate sidewall-mounted models at arbitrary angles of attack. The TDT OTT is unique because of its ability to oscillate high-inertia models (up to 65,000 lbm · in.^{2}) ±1 deg at frequencies up to 40 Hz at transonic conditions. Using the OTT, steady angles of attack and unsteady pitch oscillations can be obtained. Typically, models are oscillated at a prescribed frequency and amplitude about a mean angle of attack. The frequency response of the system is dependent on model inertia and aerodynamic loads. For the RSM, frequencies in excess of 10 Hz were demonstrated. Reference 12 contains details of the OTT design and operation.

RSM Experimental Data

The RSM data acquired during the balance test is thoroughly documented in Ref. 13. Reference 14 summarizes several HSR tests including the PAPA test, but it did not examine any of the unsteady aerodynamic data. The focus of this section will be to document the aerodynamic data acquired during OTT tests including steady and unsteady pressures. Additional experimental results and comparisons between data acquired on the OTT and data acquired on the PAPA and balance mounts are presented in Ref. 11.

OTT Database Description

The RSM/OTT database is comprised primarily of data acquired at various combinations of 2 dynamic pressures q and 10 Mach numbers M. The dynamic pressures were 100 and 150 psf, and the Mach numbers were 0.5, 0.7, 0.8, 0.9, 0.95, 0.98, 1.0, 1.02, 1.05, and 1.1. Table 1 summarizes the various combinations of mean angle of attack α_0, oscillation frequency f, and amplitude α_1 at which data were acquired. Note that at each combination of M, q, and α_0 a steady data point (i.e., $f = 0$ Hz) was acquired. The length of each time history was either 15 or 30 s depending on the frequency of oscillation. Additionally, at each combination of M and q, data were acquired during a sine sweep from 1 to 12 Hz. Other data acquired during the RSM/OTT wind-tunnel test included M, q, and α_0 conditions corresponding to the flutter points obtained from test 530 (RSM/PAPA).

Steady Data

Figure 2 shows an example of mean pressure coefficients acquired on the OTT at several fixed angles of attack ($f = 0$ Hz). The data shown in Fig. 2 are for a subsonic Mach number of 0.5, and, with the exception of the leading-edge suction peak at 30% span and

Table 1 Pitch oscillation amplitudes (α_1, ±deg) acquired for various mean angles of attack (α_0, deg) and frequency (f, Hz) combinations for test 547 (RSM/OTT)

	Pitch oscillation amplitude (α_1), deg					
α_0	$f=0$	$f=1$	$f=2$	$f=5$	$f=8$	$f=10$
−5	0	2	1	1	0.5	0.25, 0.5
−3	0	2	1	1	0.5	0.25, 0.5
0	0	2	1	1	0.5	0.25, 0.5
0	0	3	1.5	1.5	1	0.5, 1.0
3	0	2	1	1	0.5	0.25, 0.5
6	0	2	1	1	0.5	0.25, 0.5
9	0	2	1	1	0.5	0.25, 0.5
12	0	2	1	1	0.5	0.25, 0.5
15	0	2	1	1	0.5	0.25, 0.5

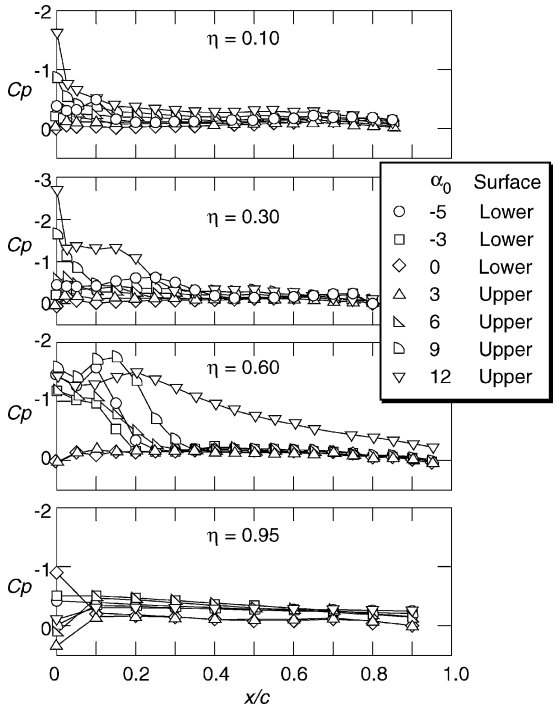

Fig. 2 Comparison of test 547 (OTT) steady pressure coefficients (suction side only) for seven angles of attack ($M = 0.50$, $q = 150$ psf).

12-deg angle of attack, all the pressure coefficients are well below C_p critical ($C_{p_{cr}} = -2.38$). Thus, none of the features in the data can be attributed to shock waves. All span stations exhibit a variation of the leading-edge suction peak with angle of attack. The most interesting features of these data can be found at 30 and 60% span. Here the effects of vortical flow can bee seen at the larger magnitude angles of attack. At 60% span, vortical flow is noted on the lower surface from the leading edge to 20% chord for −5 and −3 deg, and on the upper surface for angles of 6, 9, and 12 deg. At this Mach number the zero-lift angle of attack for the RSM is approximately 1.6 deg, and the pressures at this span station display reasonable symmetry with respect to that angle. At 30% span, vortical flow is noted for 12 deg and, to a lesser extent and further aft, vortical flow is shown in the −5-deg data. The 10 and 95% span stations exhibit no significant features with the exception of the −5-deg data at 10% span. Here, vortical flow appears to be present on the lower surface at 10% chord. The potential significance of this relative to RSM/PAPA flutter will be discussed later.

Unsteady Data

Figure 3 shows a sample of unsteady pressure data acquired during the OTT test. Magnitude of C_p at a forced frequency of 2 Hz and an oscillation amplitude of ±1 deg are shown for three angles of attack at a subsonic Mach number. High magnitudes in this type of data are generally associated with shock motion or movement of vortical flow regions. Large magnitudes are noted at the leading edge for the nonzero angles of attack. The effects of vortex motion are seen primarily at 30 and 60% span. There may be a small amount of vortex motion near the leading edge at 95% span for 6 deg, and no vortex motion is noted at 10% span. A similar comparison of transonic data including phase information is shown in Ref. 11. The transonic data show many of the same features that were found in the subsonic data. In general, the major features found in the subsonic data are moved farther aft in the transonic data.

The flutter points and boundaries for the RSM/PAPA configuration are shown in Fig. 4. Time history data were acquired at each of the flutter points. The results are plotted as dynamic pressure vs Mach number for various values of the mean angles of attack. The baseline (0-deg) flutter boundary exhibits a shallow transonic dip followed by an abrupt rise. As angle of attack becomes more negative, the boundaries shift to lower dynamic pressures and tend

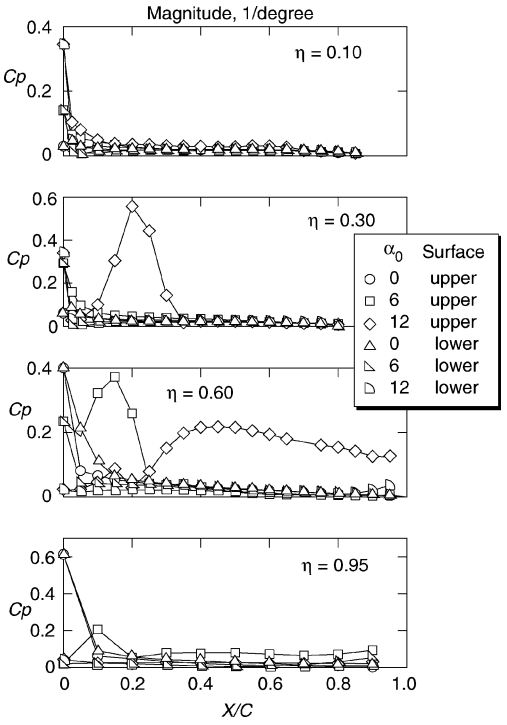

Fig. 3 Comparison of test 547 (OTT) unsteady pressure magnitudes at three mean angles of attack ($M = 0.50, q = 150$ psf, $f = 2$ Hz, $\alpha_1 = \pm 1$ deg).

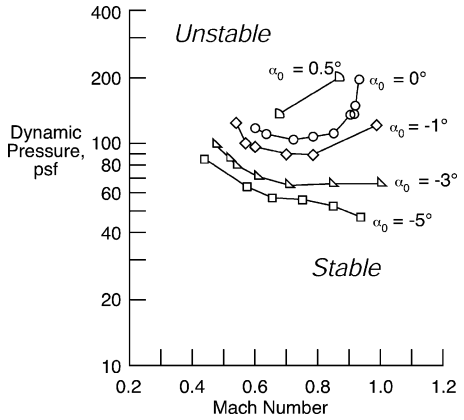

Fig. 4 Experimental flutter boundaries as a function of mean angle of attack for the RSM/PAPA configuration, no nacelles.

to flatten out. The flutter frequency for these results varied from 4.75 to 4.78 Hz. The flutter results indicate a strong dependence on angle of attack, which is unusual for thin wings at subsonic conditions.

The strong relationship between the flutter boundary and angle of attack may be due in large part to the airfoil shape on the strake portion of the wing. Whereas the outboard wing has a sharp leading edge, the strake portion of the wing has a rounded leading edge but has a relatively flat lower surface. Because of this strake geometry negative angles of attack would have a greater tendency to generate vortical flow farther forward and inboard on the lower surface of the strake than positive angles on the upper surface. This hypothesis is supported by the steady data shown in Fig. 2, where there is evidence of a lower surface strake vortex at 10% span for −5-deg angle of attack. For this span station there is no evidence of vortical flow for any of the positive angles up to 12 deg. Similarly for the 30% span there is evidence of a lower surface strake vortex at −5 and, to a lesser extent, −3 deg. At this span station, evidence of an upper-surface vortex exists only at 12 deg. The formation of the strake vortex on the lower surface as angle of attack is reduced to −5 deg would cause the center of pressure to move forward and apparently has a destabilizing effect on the flutter boundary.

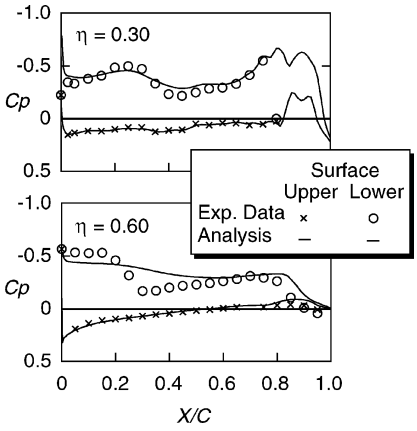

Fig. 5 Comparison of CFL3D analysis and test 547 (RSM/OTT) steady pressure coefficients ($M = 0.95$, $q = 150$ psf, $Re = 2.2 \times 10^6$ ft^{-1}, $\alpha_0 = -5$ deg).

CFD Analysis

There is significant interest in using the RSM data for validating computational methods. A primary reason for this interest is the unusual flutter boundary acquired during testing of the RSM on the PAPA. As previously mentioned, high-aspect-ratio wings with thin airfoils exhibit no variation in the flutter dynamic pressure due to moderate changes in angle of attack at subsonic conditions. This characteristic allows the use of linear flutter analysis methods based on lifting-surface theories (flat-plate models). But the flutter boundary exhibited by the RSM on the PAPA is indicative of significant nonlinear effects because the flutter boundary is a strong function of angle of attack across the Mach-number range. Therefore, because there are no shocks at subsonic conditions, the nonlinear effects must be due to vortical flow induced by the RSM's low aspect ratio, high inboard sweep, and outboard sharp leading edge. As a result of this aeroelastic sensitivity to complex flow physics, this data set poses an interesting challenge to the validation of computational methods.

CFL3Dv6 and Grid

The recently developed CFL3D version 6.0 (CLF3Dv6) CFD code is being used for the steady and unsteady analysis of the RSM wind-tunnel model. The CFL3Dv6 code solves the time-dependent conservation law form of the Reynolds-averaged Navier–Stokes equations[15] using a finite volume approach. Upwind biasing is used for the convective and pressure terms while central differencing is used for the shear stress and heat transfer terms. Implicit time advancement is used with the ability to solve steady or unsteady flows. Subiteration and multigrid capabilities are available for improved accuracy and convergence acceleration. In addition, numerous turbulence models are provided.[¶]

Data from photogrammetry, used to measure surface ordinates, was used to generate IGES models of the RSM and the 14-ft fuselage. These IGES models were then used to create grids for subsequent use in CFD analyses. The grid used in this analysis is a C-H topology grid, dimensioned at $305 \times 81 \times 49$ grid points, suitable for Navier–Stokes calculations.

Computational Results and Comparisons with Experimental Data

A comparison of computational and experimental steady pressure distributions at a Mach number of 0.95, $Re = 2.2 \times 10^6$ ft^{-1}, and $\alpha_0 = 3$, 6, −3, and −5 deg is shown in detail in Ref. 11. All results were computed using the Spalart–Allmaras turbulence model. This section will show a sample of these steady comparisons.

Figure 5 presents the comparison for −5-deg angle of attack. Only two of the four span stations are shown. The vortical flow near the

[¶]Data available online at http://cfl3d.larc.nasa.gov/Cfl3dv6/cfl3dv6.html [cited 7 October 2003].

quarter chord at the 30% span station has been captured by the computations. The large variations in the computational results at the 30% span station near the trailing edge are due to surface variations associated with the trailing-edge control surface. The control surface was not instrumented with pressure ports so there are no pressure measurements available for this region. The comparison with the outboard span stations is poor, especially at the 60% station. Improved grid resolution is needed for the outboard span stations to capture the vortical flow phenomena in that region.[16]

A refined grid was generated and steady calculations performed and presented in Ref. 17. These results provided only a marginal improvement in the analysis test correlation in the vortical flow regions especially at 60% span. Some unsteady calculations have also been performed for the RSM on the OTT. These results are presented in Refs. 17 and 18.

Summary

A large database of steady, unsteady, and flutter wind-tunnel data has been obtained for three configurations based on an HSCT design: the RSM on a balance, the RSM on a PAPA, and the RSM on the OTT. The database covers an extensive Mach-number range from subsonic to low supersonic with a special emphasis on transonic conditions. The RSM was highly instrumented and the acquired database represents one of the largest aerodynamic and aeroelastic databases available. Examples of steady and unsteady pressure data were shown. The flutter behavior of the RSM on the PAPA mount was examined. Preliminary CFD analyses were performed and compared with experimental data. All of the RSM wind-tunnel data are available for public distribution.

References

[1]Corliss, J. M., and Cole, S. R., "Heavy Gas Conversion of the NASA Langley Transonic Dynamics Tunnel," *Proceedings of the 20th Advanced Measurements and Ground Testing Technology Conference*, NASA, Langley Research Center, Hampton, VA, June 1998.

[2]Cole, S. R., and Rivera, J. A., Jr., "The New Heavy Gas Testing Capability in the NASA Langley Transonic Dynamics Tunnel," *Royal Aeronautical Society Wind Tunnels and Wind Tunnel Test Techniques Forum*, The Royal Aeronautical Society, No. 4, Cambridge, England, UK, April 1997.

[3]Ruiz-Calavera, L. P., Bennett, R., Fox, J., Huang, X., Kaynes, I., Galbraith, R., Henshaw, M., Naudin, P., Geurts, E., Löser, T., and Tamayama, M., "A New Compendium of Unsteady Aerodynamic Test Cases for CFD: Summary of AVT WG-003 Activities," *International Forum on Aeroelasticity and Structural Dynamics*, Confederation of European Aerospace Societies (CEAS) and the AIAA, NASA Langley Research Center, Hampton, VA, June 1999.

[4]Bennett, R. M., Eckstrom, C. V., Rivera, J. A., Jr., Dansberry, B. E., Farmer, M. G., and Durham, M. H., "The Benchmark Aeroelastic Models Program: Description and Highlights of Initial Results," NASA TM 104180, April 1991.

[5]Durham, M. H., Keller, D. F., Bennett, R. M., and Wieseman, C. D., "A Status Report on a Model for Benchmark Active Controls Testing," AIAA Paper 91-1011, April 1991.

[6]Rivera, J. A., Jr., Dansberry, B. E., Bennett, R. M., Durham, M. H., and Silva, W. A., "NACA0012 Benchmark Model Experimental Flutter Results with Unsteady Pressure Distributions," NASA TM 107581, April 1992.

[7]Rivera, J. A., Jr., Dansberry, B. E., Durham, M. H., Bennett, R. M., and Silva, W. A., "Pressure Measurements on a Rectangular Wing with a NACA0012 Airfoil During Conventional Flutter," NASA TM 104211, July 1992.

[8]Dansberry, B. E., Durham, M. H., Bennett, R. M., Turnock, D. L., Silva, W. A., and Rivera, J. A., Jr., "Physical Properties of the Benchmark Models Program Supercritical Wing," NASA TM 4457, Sept. 1993.

[9]Scott, R. C., Hoadley, S. T., Wieseman, C. D., and Durham, M. H., "The Benchmark Active Controls Technology Model Aerodynamic Data," *Journal of Guidance, Control, and Dynamics*, Vol. 23, No. 5, 2000, pp. 914–921; also AIAA Paper 97-0829, Jan. 1997.

[10]Schuster, D. M., Spain, C. V., Turnock, D. L., Raush, R. D., Hamounda, M.-N., Vogler, W. A., and Stockwell, A. E., "Development, Analysis, and Testing of the High Speed Research Flexible Semispan Model," NASA CR 1999-209556, Sept. 1999.

[11]Scott, R. C., Silva, W. A., Florance, J. R., and Keller, D. F., "Measurement of Unsteady Pressure Data on a Large HSCT Semispan Wing and Comparison with Analysis," AIAA Paper 2002-1648, April 2002.

[12]Piatak, D. J., and Cleckner, C. S., "A New Forced Oscillation Capability for the Transonic Dynamics Tunnel," AIAA Paper 2002-0171, Jan. 2002.

[13]Schuster, D. M., and Rausch, R. D., "Transonic Dynamics Tunnel Force and Pressure Data Acquired on the HSR Rigid Semispan Model," NASA CR 1999-209555, Sept. 1999.

[14]Silva, W. A., Keller, D. F., Florance, J. R., Cole, S. R., and Scott, R. C., "Experimental Steady and Unsteady Aerodynamic and Flutter Results for HSCT Semispan Models," AIAA Paper 2000-1697, April 2000.

[15]Kris, S. L., Biedron, R. T., and Rumsey, C. L., "CFL3D User's Manual Version 5.0," NASA-TM 1998-208444, June 1998.

[16]Bartels, R. E., and Gatski, T. B., "Prediction of Transonic Vortex Flows Using Linear and Nonlinear Turbulent Eddy Viscosity Models," NASA-TM 2000-210282, May 2000.

[17]Scott, R. C., and Silva, W. A., "Pitch Oscillation Data and Analysis for a Large HSCT Semispan Wing," *AIAA/CEAS International Forum on Aeroelasticity and Structral Dynamics*, IFASD-US-38, Confederation of European Aerospace Societies (CEAS) and the AIAA, NASA Langley Research Center, Hampton, VA, Amsterdam, June 2003.

[18]Hong, M. S., Kuruvila, G., Bhatia, K. G., SenGupta, G., and Kim, T., "Evaluation of CFL3D for Unsteady Pressure and Flutter Predictions," AIAA Paper 2003-1932, April 2003.

Effects of Reynolds Number on Characteristics of Fixed and Rotary Wings

S. Sunada*
Osaka Prefecture University, Osaka 599-8531, Japan
and
K. Kawachi†
University of Tokyo, Tokyo 113-8656, Japan

Nomenclature

AR	=	aspect ratio
ARe	=	effective aspect ratio
b	=	number of wings
C_D	=	coefficient of drag of a wing, as indicated by Eq. (7)
C_{Dp}	=	profile drag, as indicated by Eq. (4)
C_d	=	coefficient of drag of an airfoil, $C_d(C_\ell = 0) + \delta_1(\alpha - \alpha_0) + \delta_2(\alpha - \alpha_0)^2$
C_L, C_ℓ	=	coefficients of lift of a wing and an airfoil, respectively
$C_{L\alpha}, C_{\ell\alpha}$	=	lift slope of a wing and an airfoil, respectively
C_T, C_Q	=	thrust and torque coefficients, respectively
c	=	chord length
R	=	diameter of a rotary wing
$\bar{R}$	=	ratio between profile drag proportional to $(\alpha - \alpha_0)^2$ and induced drag and induced drag, as indicated by Eq. (12)
Re	=	Reynolds number
r	=	spanwise position of a rotary wing
U	=	forward speed
W/S	=	wing loading
w	=	sinking speed
α	=	geometrical angle of attack

Received 27 May 2003; revision received 12 June 2003; accepted for publication 30 July 2003. Copyright © 2003 by the American Institute of Aeronautics and Astronautics, Inc. All rights reserved. Copies of this paper may be made for personal or internal use, on condition that the copier pay the $10.00 per-copy fee to the Copyright Clearance Center, Inc., 222 Rosewood Drive, Danvers, MA 01923; include the code 0021-8669/03 $10.00 in correspondence with the CCC.

*Associate Professor, Department of Aerospace Engineering, Graduate School of Engineering; sunada@aero.osakafu-u.ac.jp.

†Professor, Department of Aeronautics and Astronautics. Associate Fellow AIAA.